Turkish Journal of Chemistry
http://journals.tubitak.gov.tr/chem/
Research Article

Turk J Chem
(2015) 39: 1232 – 1246

doi:10.3906/kim-1506-32

Efficient C–C cross-coupling reactions by (isatin)-Schiff base functionalized magnetic nanoparticle-supported Cu(II) acetate as a magnetically recoverable catalyst

Seyedeh Simin MIRI[1], Mehdi KHOOBI[2,3], Fatemeh ASHOURI[4], Farnaz JAFARPOUR[1], Parviz RASHIDI RANJBAR[1], Abbas SHAFIEE[2,*]

[1]School of Chemistry, College of Science, University of Tehran, Tehran, Iran
[2]Department of Medicinal Chemistry, Faculty of Pharmacy and Pharmaceutical Sciences Research Center, Tehran University of Medical Sciences, Tehran, Iran
[3]Medical Biomaterials Research Center, Tehran University of Medical Sciences, Tehran, Iran
[4]Department of Applied Chemistry, Faculty of Pharmaceutical Chemistry, Pharmaceutical Sciences Branch, Islamic Azad University, Tehran, Iran

Received: 14.06.2015 • **Accepted/Published Online:** 07.09.2015 • **Printed:** 25.12.2015

Abstract: Copper catalysts were simply fabricated through surface modification of superparamagnetic iron nanoparticles with indoline-2,3-dione(isatin)-Schiff-base and interaction with Cu from low-cost commercially available starting materials. Catalysts were characterized using atomic absorption spectrophotometry, Fourier transform infrared spectroscopy, X-ray diffraction, thermogravimetric analysis, vibrating sample magnetometry, UV/Vis spectroscopy, scanning electron microscopy, and transmission electron microscopy. These catalysts showed high efficiency for phosphine-free Mizoroki–Heck and Suzuki–Miyaura cross-coupling reactions with good diversity and generality. The catalysts could be easily recovered and reused several times without a significant loss in their catalytic activity and stability.

Key words: Copper, coupling, magnetic nanoparticles, catalyst, Schiff base

1. Introduction

C–C bond formation is one of the most commonly employed chemical transformations generally used in both academic[1] and industrial chemistry.[2] Mizoroki–Heck and Suzuki–Miyaura cross-coupling reactions are the most widely used methods for extensive production of key intermediates during preparation of natural,[3] nonnatural,[4] and bioactive compounds.[5,6] Although homogeneous palladium complexes as conventional catalysts in cross-coupling reactions have shown high reaction rates, suitable turnover numbers, and sometimes perfect selectivity and yield, these types of catalysts suffer from the problem of recycling of the catalyst as well as instability during reaction at high temperatures.[7,8] Recoverability and reusability of the catalyst are a challenge from environmental and economic points of view, especially when precious metal catalysts are used. In this regard, magnetic nanoparticles (MNPs) can particularly meet this challenge due to their ability to easily separate from liquid reaction media by an external magnetic field. Among various MNPs, magnetite (Fe_3O_4) has attracted considerable interest and has applications in various fields due to its large surface-to-volume ratio, biocompatibility, nontoxicity, ease of synthesis, and surface functionalization.[9,10]

*Correspondence: shafieea@tums.ac.ir

In addition, the type of ligand in transition metal cross-coupling is one of the pivotal factors determining catalytic performance. Conventionally, homogeneous palladium/phosphine complexes were used in Mizoroki–Heck and Suzuki–Miyaura reactions. However, limiting aspects of palladium catalysts like high cost and toxicity have limited their immense applications on industrial scales.[11] In recent years, copper catalytic systems have been attracting more attention because of their low costs, biocompatibility, and increased catalytic ability in comparison with palladium and other frequently used systems for catalyzing cross-coupling reactions.[12–14]

Since ligands can influence the selectivity and reactivity of transformations, careful choice of ligand is required for functionalization of catalyst supports.[15–21] Among the various applied ligands, nitrogen-containing ligands and especially Schiff bases as potent organic ligands in coordination chemistry play an important role in tuning the electronic properties of metal ions in complexes.[22]

Since isatin-based Schiff base ligands have shown variable denticities toward several metal ions,[23,24] we were encouraged to fabricate a new magnetic copper Schiff base complex via surface modification of superparamagnetic iron nanoparticles with an indoline-2,3-dione (isatin)-Schiff base and subsequent ligand coordination with Cu (Scheme).

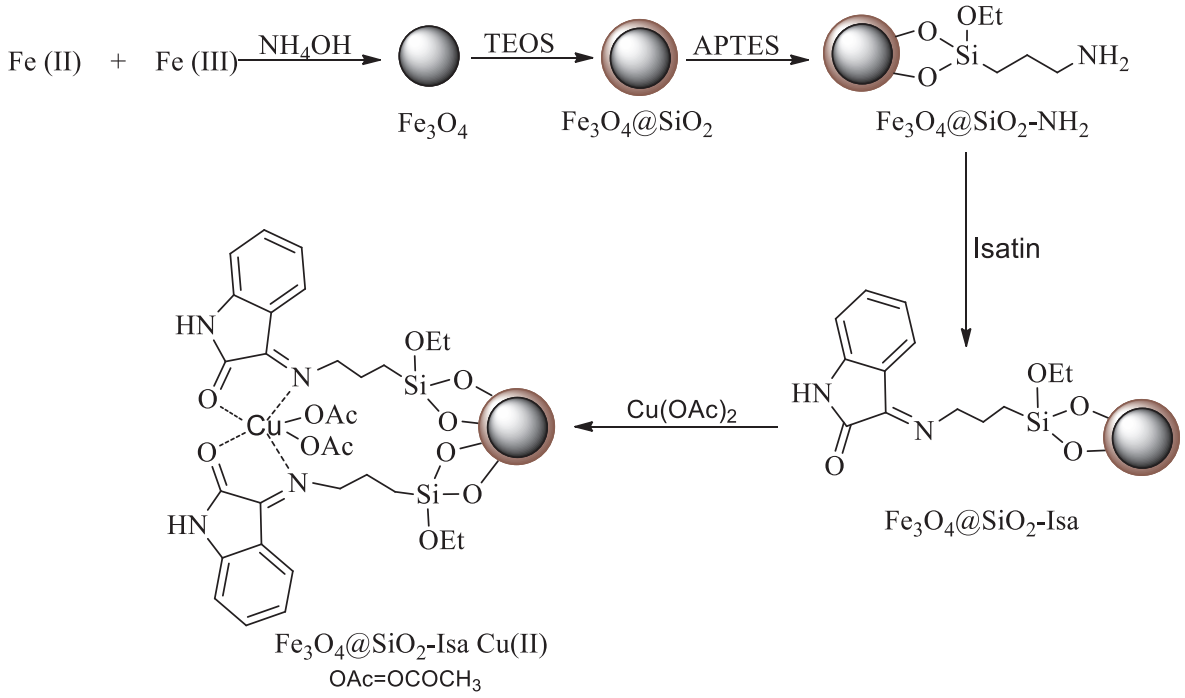

Scheme. The consecutive steps for preparing copper catalyst.

2. Results and discussion

2.1. Catalyst preparation and characterization

The sequential steps for stabilizing Cu(II) ions by indoline-2,3-dione (isatin)-Schiff base containing MNPs is shown in the Scheme. Condensation reaction of Fe_3O_4@SiO_2–NH_2 with isatin (Isa) was used to produce a suitable interaction capacity of N–O Schiff base and metal species. An inductive coupled plasma-atomic emission spectrometry (ICP) analyzer was used to determine the content of Cu and revealed the presence of 0.17 mmol/g. Fourier transform infrared (FT-IR) analysis was used to confirm the modification of the magnetite

surface with functional groups and also metal anchoring on the nanocomposite. The FT-IR spectra of Fe_3O_4, Fe_3O_4@SiO_2–NH_2, Fe_3O_4@SiO_2–Isa, and Fe_3O_4@SiO_2–Isa Cu(II) are shown in Figure 1. The absorption band at 584–633 cm^{-1} in the MNPs is attributed to the stretching vibration of Fe–O, and the peak at 3415 cm^{-1} is assigned to the stretching vibrations of Fe–OH groups on the surface of the MNPs. The strong broad band at 1000–1100 cm^{-1} corresponds to the stretching vibration of the Si–O–Si group and confirmed the silica coating on the surface of Fe_3O_4. The bands at 2940 and 1446 cm^{-1} could be ascribed to the stretching vibrations of C–H and C–N bonds, respectively (Figure 1, line b). After condensation of isatin with amine groups of Fe_3O_4@SiO_2–NH_2, more peaks appeared at 1714 and 1621 cm^{-1}, which are due to the stretching vibration of carbonyl and C=N bands, respectively. The FT-IR spectrum of the Cu(II) catalyst shows a red shift in the carbonyl bond at a lower frequency (1708 cm^{-1}) in comparison with the band for Fe_3O_4@SiO_2–Isa. The stretching bands correspond to the carbonyl and C=N bonds of complexes show a red shift compared with the Schiff base (Fe_3O_4@SiO_2–Isa) and appear at a lower frequency (Figure 1, line c in comparison with line d). This could be attributed to the coordination of the carbonyl and C=N bands with copper ions.[25,26]

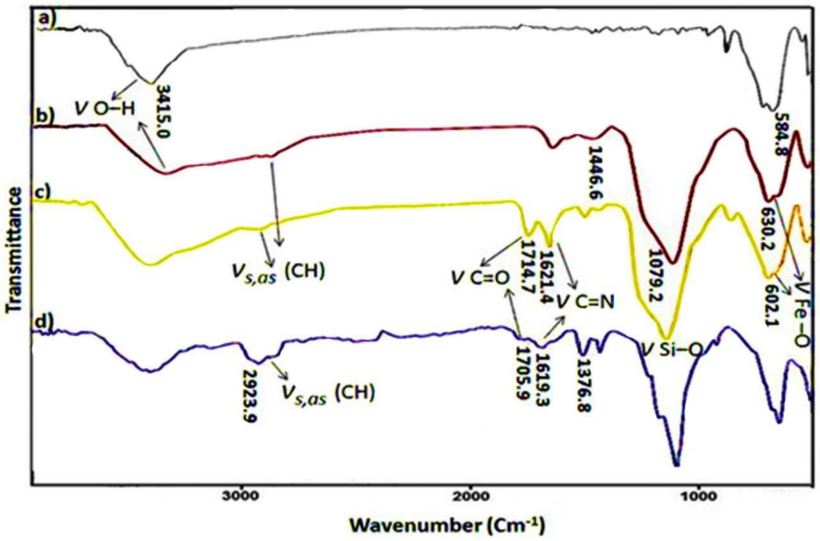

Figure 1. FT-IR spectra of (a) Fe_3O_4, (b) Fe_3O_4@SiO_2–NH_2, (c) Fe_3O_4@SiO_2–Isa, and (d) Fe_3O_4@SiO_2–Isa Cu(II).

The thermogravimetric analysis (TGA) curves of Fe_3O_4, Fe_3O_4@SiO_2–Isa, and copper catalyst are shown in Figure 2. Weight loss observed during heating from 50 to 200 °C could be ascribed to the loss of physisorbed water and other solvents on the particles during nanocatalyst procurement (Figure 2, line a). Thermal decomposition of the immobilized Schiff base and corresponding complexes revealed the continuous weight loss of organic moiety absorbed on the particle surface in the temperature range of 200–600 °C. As illustrated in Figure 2 (line b), the amount of Schiff base ligand loading on the surface of the MNPs is approximately 8%. As a result, the nanocatalyst is stable up to at least 200 °C.

The X-ray powder diffraction (XRD) patterns of naked Fe_3O_4 and catalyst are shown in Figure 3. The XRD results showed that diffraction peaks at 2θ of 30.09°, 35.7°, 43.3°, 53.85°, 57.31°, and 62.97° correlated to diffraction of (220), (311), (400), (422), (511), and (440) of the Fe_3O_4 nanoparticles were found in all samples. Therefore, the multiple steps of catalyst preparation did not change the crystal structure of the Fe_3O_4 cores.

The new peaks at $2\theta = 40.33°$, $59.57°$, and $66.19°$ corresponding to the (111), (202), and (311) planes of Cu^{+2} indicated the existence of Cu^{+2} in the catalyst.[27] The broad peak that appeared at $2\theta = 21$–$25°$ in both catalysts is related to the amorphous silica shell on the surface of the MNPs[28] The average crystallite sizes of MNPs were estimated as 13.5 nm using the Scherrer equation.

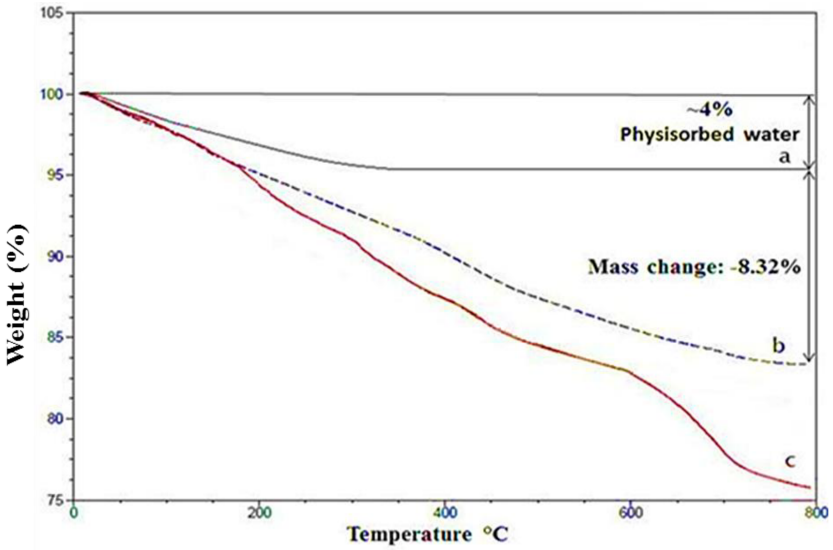

Figure 2. TGA curves of (a) Fe_3O_4, (b) Fe_3O_4@SiO_2–Isa, and (c) Fe_3O_4@SiO_2–Isa Cu(II) catalyst.

Diffuse reflectance spectroscopy (DRS) was used for corroboration of oxidation states of Cu species in the structure. The spectrum of Fe_3O_4@SiO_2–Isa Cu(II) shows higher absorption at ~700–800 nm compared to Fe_3O_4@SiO_2–Isa, which can be assigned to the Cu(II) d–d transition intensity in the presence of Fe_3O_4@SiO_2–Isa Cu(II) (Figure 4).[29–32] The Fe_3O_4@SiO_2–Isa Cu(II) and Fe_3O_4@SiO_2–Isa indicated a peak at 220 nm, which can be attributed to the existence of the magnetic core.

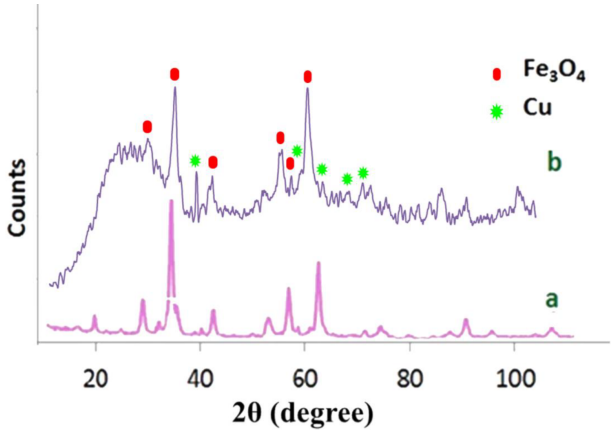

Figure 3. XRD pattern of (a) Fe_3O_4 and (b) Fe_3O_4@SiO_2–Isa Cu(II) catalyst.

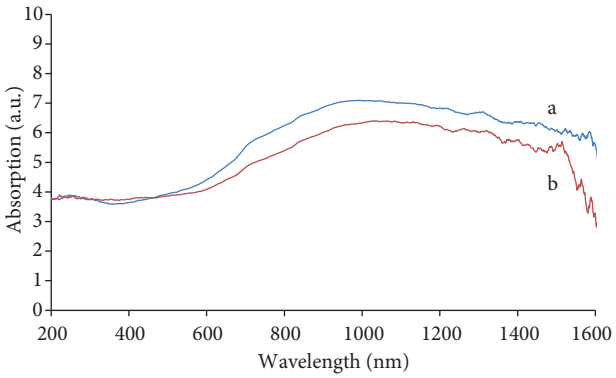

Figure 4. DRS pattern of Fe_3O_4@SiO_2–Isa Cu(II) catalyst (a) and Fe_3O_4@SiO_2–Isa (b).

The magnetic feature of Fe_3O_4 MNPs and Fe_3O_4@SiO_2–Isa was measured with a VSM (vibrating sample magnetometry) instrument (Figure 5, lines a and b, respectively). Base on the hysteresis loop, magnetic

saturation of Fe_3O_4 MNPs and Fe_3O_4@SiO_2–Isa is 46.5 and 37.5 emu g^{-1}, respectively. The decrease in mass saturation magnetization of Fe_3O_4@SiO_2–Isa could be ascribed to the nonmagnetic silica and organic moieties. Although the σ_s values of the Fe_3O_4@SiO_2–Isa are decreased, the superparamagnetic properties of nanoparticles have been still been preserved and the absence of remanence magnetization and coercivity confirm this. The catalyst could be efficiently isolated magnetically from the solution and reused for several runs (Figure 5).

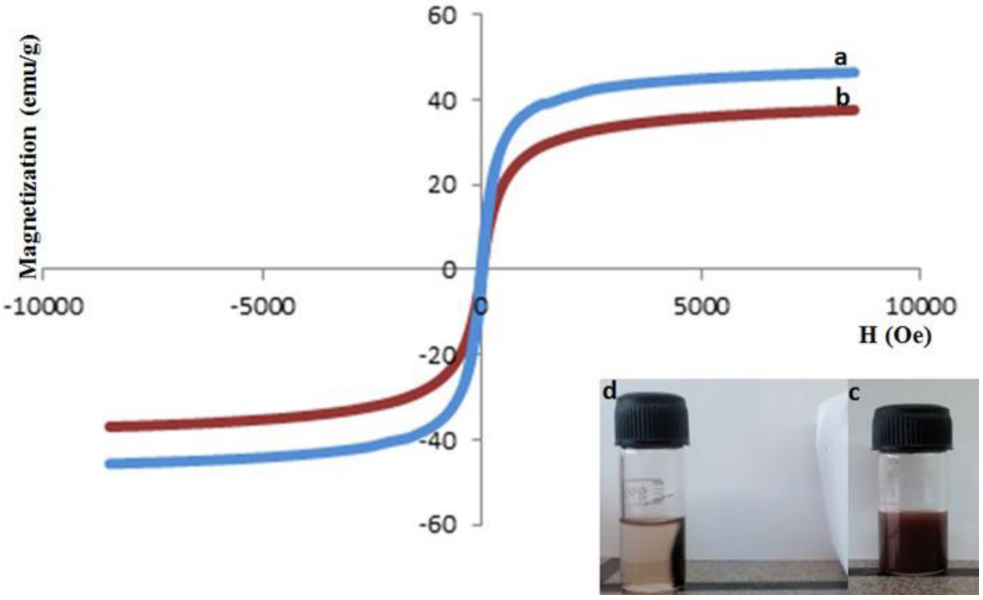

Figure 5. VSM curve of Fe_3O_4 MNPs (a) and Fe_3O_4@SiO_2–Isa (b); reaction mixture (c) and isolation of catalyst by external magnet (d).

The SEM and TEM images of the catalysts are presented in Figures 6a–6c. According to these images, most of particles have a narrow size distribution (the inset histogram of Figure 6c) with quasi-spherical shape. The mean diameter of the nanoparticles was about 12 nm. These results are consistent with the average crystallite sizes estimated from XRD by using Scherrer's equation. Energy dispersive X-ray spectroscopy (EDS) spectra were also used to determine the elemental composition of catalysts. EDS spectra of Fe_3O_4@SiO_2–Isa Cu(II) clearly demonstrate the presence of Cu, Fe, and Si as well as other elements attributed to the organic moiety. The presence of these signals confirms the successful preparation of catalyst and copper loading (Figure 6d).

2.2. Catalytic activity of catalysts in Mizoroki–Heck coupling reaction

The catalytic activity of the as-prepared Cu catalysts was investigated in Mizoroki–Heck coupling reactions. As a model reaction, the coupling of iodobenzene and methyl acrylate was screened in order to find the optimized conditions (Table 1). A careful view into the C–C cross-coupling reaction process indicates that the reaction conditions have affected the yield of the Mizoroki–Heck reaction.[33,34] The influence of different experimental parameters, such as reaction time and amount of catalyst and base, were also optimized in the model reaction. Among them, the best condition was obtained in the presence of Et_3N as base and DMF as solvent (Table 1, entry 8). Using Cs_2CO_3 as a strong base caused a decrease in the yield of the desirable stilbene due to the

formation of homocoupling products (Table 1, entry 4).[35] The results showed that 1,4-dioxane and MNPs are also effective (Table 1, entries 10 and 14). The same results were also obtained when the amount of the catalyst was decreased to 0.33 mol% and temperature was decreased to 80 °C (Table 1, entry 18). It was noted that, as expected, temperature had a noteworthy effect on the effectiveness of the present catalytic system.

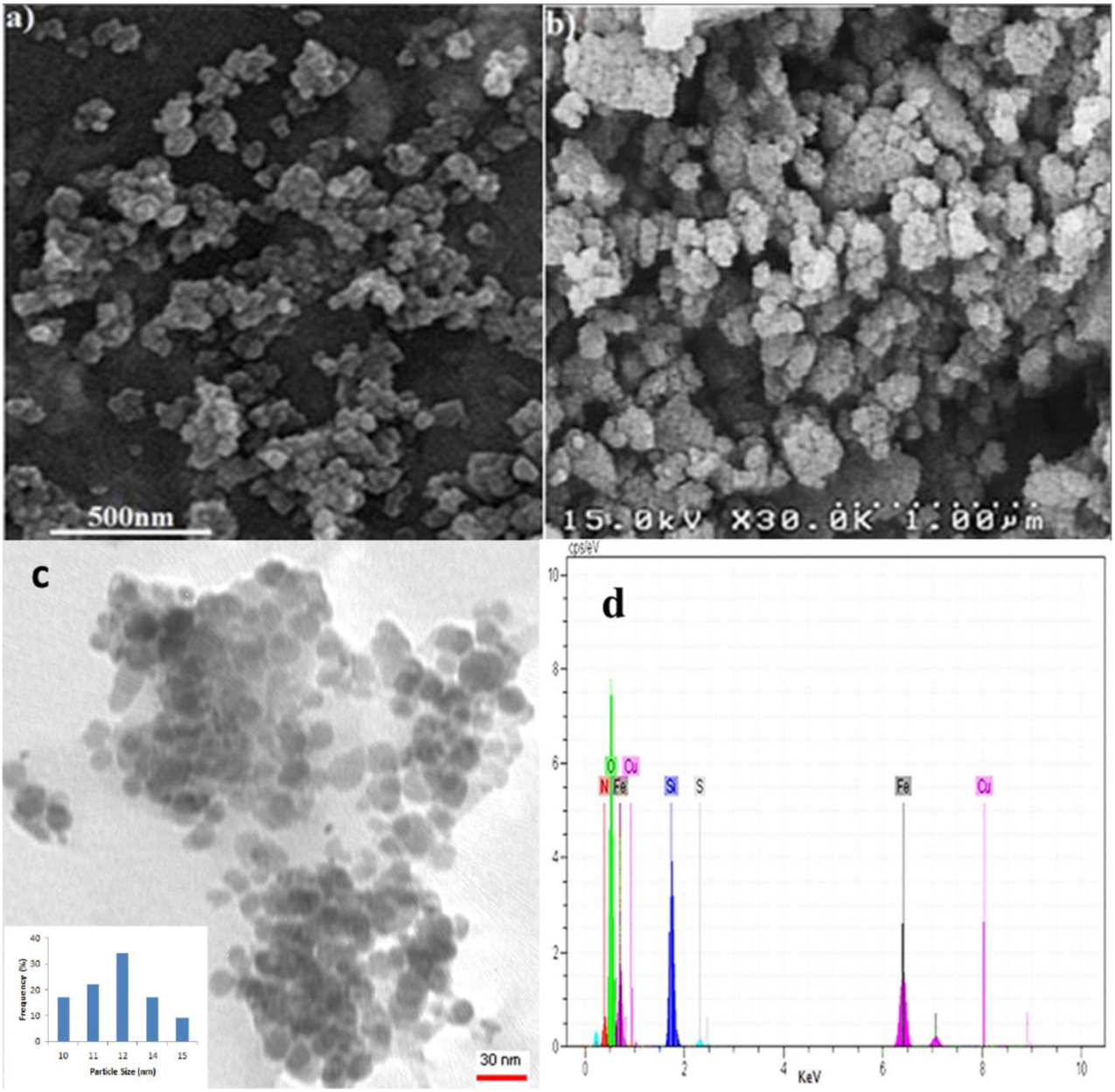

Figure 6. SEM images of Fe_3O_4 (a) and Fe_3O_4@SiO_2–Isa Cu(II) (b); TEM image and particle size distribution histogram of Fe_3O_4@SiO_2–Isa Cu(II) catalyst (particle size: 12 nm) (c); and EDS of Fe_3O_4@SiO_2–Isa Cu(II) catalyst (d).

Because good yield of the product was acquired at 100 °C, a variety of iodobenzenes and alkenes including either aromatic or aliphatic alkenes with electron-donating or electron-withdrawing substitution were

investigated under the optimized reaction conditions (100 °C). It was observed that the system for the coupling reaction of aryl halides with alkenes can be adopted for the catalytic active and regioselective coupling (Table 2).

Table 1. Optimization of reaction condition for Heck coupling reaction of methylacrylate with iodobenzene in the presence of Fe_3O_4@SiO_2–Isa Cu(II) catalyst.[a]

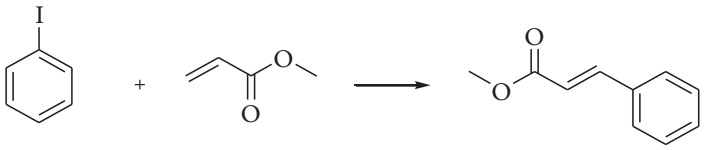

Entry	Base	Solvent	Conversion (%)[b]
1	Na_2CO_3	DMF	91
2	KH_2PO_4	DMF	50
3	Na_2HPO_4	DMF	30
4	Cs_2CO_3	DMF	Trace
5	NaOAc	DMF	-
6	DABCO	DMF	-
7	K_2CO_3	DMF	98
8	NEt_3	DMF	100
9	$(CH_3)_3COK$	DMF	-
10	NEt_3	NMP	100
11	NEt_3	DMF	100
12	NEt_3	PEG	80
13	NEt_3	EtOH	80
14	NEt_3	1,4-Dioxane	100
15	NEt_3	Mesitylene	Trace
16	NEt_3	Ethylene glycol	Trace
[c]17	NEt_3	DMF	100
[d]18	NEt_3	DMF	90
[e]19	NEt_3	DMF	100

[a] Reaction conditions: iodobenzene (1.0 mmol), methylacrylate (1.1 mmol), base (2.0 mmol), solvent (5.0 mL), 120 °C, 12 h, copper catalyst (0.82 %mol); [b] Checked by GC analysis; [c] Copper catalyst (0.33 %mol), 100 °C; [d] Copper catalyst (0.33 %mol), 80 °C; [e] 100 °C, 8 h.

2.3. Catalytic activity of the copper catalyst in Suzuki–Miyaura coupling reaction

The efficiency of the Fe_3O_4@SiO_2–Isa Cu(II) catalyst in Mizoroki–Heck coupling reaction led us to study the potential of this catalyst in the Suzuki–Miyaura cross-coupling reactions of aryl halides and arylboronic acids. In order to optimize the reaction condition, coupling of 4-iodotoluene and 4-methoxyphenylboronic acid was selected as the model reaction. Influence of different bases and solvents as well as the amount of the catalyst, temperature, and time of the reaction were also investigated. The results showed that the model reaction can be promoted in NMP and DMF with high yield (Table 3, entries 1 and 2). Due to the importance of green solvent application in organic reactions, we examined the performance of ethanol as a green solvent in the model reaction. Fortunately, excellent yield was obtained in the presence of K_2CO_3 as the base in ethanol solvent (Table 3, entry 3). However, addition of water slightly declined the yield of the reaction in comparison with ethanol. The effects of different bases such as NEt_3, DABCO (1,4-diazabicyclo[2.2.2]octane), KH_2PO_4,

Table 2. The copper catalyzed Mizoroki–Heck coupling reactions of various aryl iodides with terminal alkenes. [a]

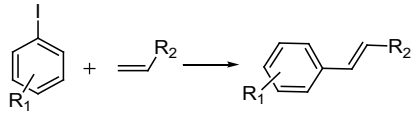

Entry	Aryl iodide	Olefin	Product	Time (h)	Conversion[b] (%)	Selectivity[b] (%)
1			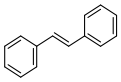	12	90	86
2			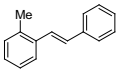	12	96	90
3			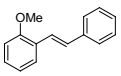	15	65	75
4			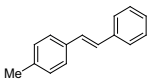	12	97	90
5			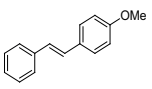	15	78	95
6			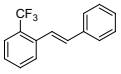	8	91	100
7			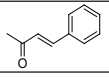	8	100	50
8			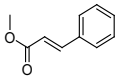	8	100	100
9			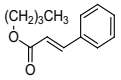	8	76	80
10			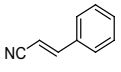	8	100	90
11		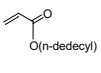	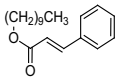	8	90	90
12			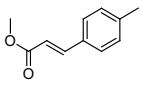	8	72	90
13			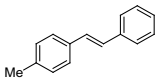	12	55	70

[a] Reaction conditions: the reactions were done in the present of copper catalyst (0.33 mol%) in the coupling reaction of aryl iodide (1.0 mmol), alkene (1.1 mmol), and NEt_3 (2.0 mmol) in DMF (5.0 mL) at 100 °C in a sealed tube; [b] GC conversion.

$(CH_3)_3COK$, and Na_2CO_3 were also studied. The best result was obtained by 0.33 mol% copper catalyst in the presence of K_2CO_3 in ethanol at 70 °C for 5h (Table 3, entry 11). Changing the amount of catalyst and temperature did not show meaningful improvement in the yield of the reaction.

Table 3. Optimization of effective factors in Suzuki–Miyaura cross-coupling reaction catalyzed by immobilized copper complex.[a]

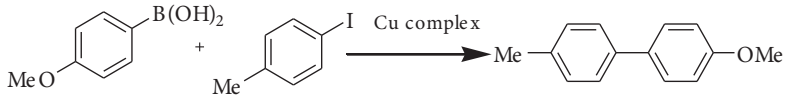

Entry	Solvent	Base	Time (h)	Conversion[b] (%)
1	DMF	K_2CO_3	12	92
2	NMP	K_2CO_3	12	90
3	EtOH	K_2CO_3	12	94
4	EtOH	KH_2PO_4	12	Trace
5	EtOH	$(CH_3)_3COK$	12	75
6	EtOH	Na_2CO_3	12	90
7	EtOH	NEt_3	12	Trace
8	EtOH	DABCO	12	75
9	EtOH:H_2O (1:1)	K_2CO_3	12	55
10	EtOH	K_2CO_3	5	94
11	EtOH	K_2CO_3	5	94[c]

[a] Reaction conditions: 4-iodotoluene (1.0 mmol), 4-methoxyphenylboronic acid (1.2 mmol), base (2.0 mmol), solvent (5 mL), Fe_3O_4@SiO_2–Isa Cu(II) catalyst (0.82 mol%), 70 °C in a sealed tube; [b] Determined by GC; [c] Copper catalyst 0.33 mol%.

The couplings between various aryl halides and arylboronic acids were investigated. As indicated in Table 4, good to excellent yields were obtained for various substrates. The reaction progressed reasonably well with bromobenzene to afford the stilbene in good yield (70%) (Table 4, entry 2). Thus, the Fe_3O_4@SiO_2–Isa Cu(II) catalyst is efficient for Suzuki–Miyaura cross-coupling reaction.

To evaluate the efficiency and stability of the catalysts during several runs, our study was concentrated on the recyclability and reusability of these catalysts. After each catalytic run, catalysts were easily recovered by a magnetic field, washed repeatedly with aqueous methanol, and dried under a vacuum at 50 °C to be checked in the next run. Leaching tests after each catalytic run in iodobenzene and methylacrylate coupling as a model reaction under optimized conditions revealed that the amount of Cu leached from the heterogeneous catalyst was negligible (less than 0.2 ppm) as determined by ICP-AES of the clear filtrate. This result shows that there is no contribution from homogeneous catalysis of active Cu species leaching into the reaction solution.

A hot filtration test was also conducted to confirm that the reaction was indeed catalyzed by Cu heterogeneous catalyst instead of free Cu. After the first catalytic reaction, the catalyst was simply separated from the reaction mixture by an external magnet. The fresh reagents were then added to the filtrated solution. The resulting mixture was stirred at 100 °C. The conversion was negligible after adequate time (8 h). These results confirmed that the coupling reaction could only proceed in the presence of the solid catalyst, and there was no contribution from leached Cu species in the liquid phase.

Efforts were directed toward the study of recycling of such catalytic systems using the Mizoroki–Heck reaction of iodobenzene with methyl acrylate. The supported catalysts were recovered by a magnetic field

Table 4. The Suzuki–Miyaura cross-coupling reactions of aryl halides with phenylboronic acids in the present of Fe_3O_4@SiO_2–Isa Cu(II) catalyst.[a]

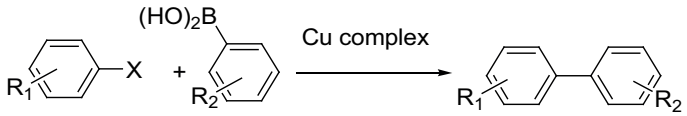

X:Br, I

	R_1	R_2	Aryl halide	Product	Conversion[b] (%)
1	4-Me	4-OMe	Br	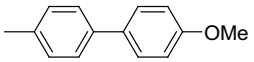	35
2	H	4-OMe	Br	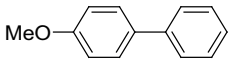	70
3	H	4-OMe	I	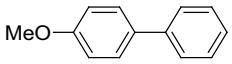	99
4	4-Me	3-NO_2	I	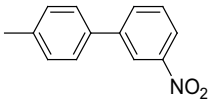	91
5	4-OMe	4-OMe	I	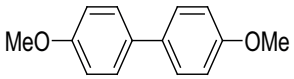	99
6	2-Me	4-OMe	I	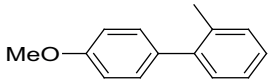	94
7	2-CF_3	4-OMe	I	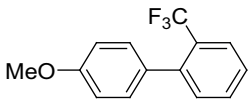	85
8	2-Me	4-OMe	Br	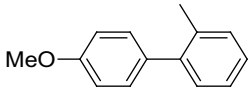	40
9	4-OMe	H	I	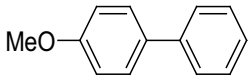	92
10	2-OMe	H	I	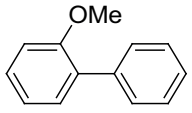	85
11	2-OMe	4-OMe	I	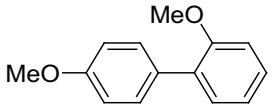	99
12	4-Me	4-OMe	I	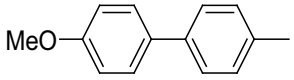	94

[a] Reaction conditions: aryl halide (1.0 mmol), phenyl borinic acid (1.2 mmol), K_2CO_3 (2.0 mmol), Cu catalyst (0.33 mol%), EtOH (5 mL), 70 °C, 5 h; [b] Determined by GC.

for the next reaction, washed with aqueous methanol, and dried under vacuum at 50 °C to reactivate the catalysts for the next run. The model reaction under the optimized conditions mentioned above was run for five consecutive cycles repeating the regeneration process of two catalysts. There was a drop in the yield of the reaction catalyzed by copper catalyst after the fourth cycle, which could be attributed to the leaching of copper ions (Figure 7). ICP analysis result showed 6% deterioration of copper content at the fifth cycle. Lower stability of copper catalyst for Suzuki–Miyaura reaction may be attributed to the metal leaching due to the effect of protic solvent and high temperature of the reaction media.[36]

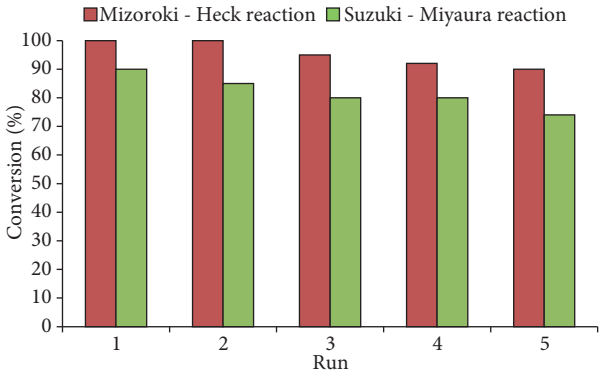

Figure 7. Recovery of Fe_3O_4@SiO_2–Isa Cu(II) catalyst in Heck and Suzuki coupling reactions.

Considering published reports in this field, it has been revealed that some heterogeneous copper-catalyzed cross-coupling reactions suffer from elevated temperature to obtain desirable results (Table 5, entries 2–4),[12,37,38] low yield under the optimum conditions,[39] or costly and difficult procedures[40,41] for catalyst preparation (Table 5, entry 5, and Table 6, entry 2). In this study, not only was an efficient hybrid magnetic copper catalyst conveniently prepared for the C–C cross-coupling reactions with a low level of the catalyst, but it also gave the desired products in moderate to excellent yields without using bimetallic systems (Table 5, entry 6, and Table 6, entries 4–6).[42−44]

Table 5. Comparison of catalytic activity of various heterogeneous catalysts in the Mizoroki–Heck cross-coupling reactions.

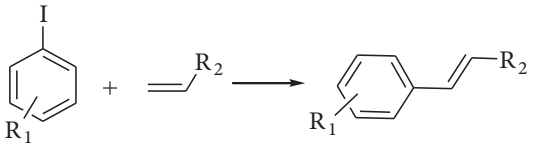

Entry	R_1	R_2	Catalyst	Temperature (°C)	Yield (%)/ Time (h)	Ref.
1	H	Ph	Fe_3O_4@SiO_2–Isa Cu(II)	100	90[a]/8	This work
2	H	COOBu	Copper bronze	130	70/24	12
4	H	Ph	Si-NH_2-$Cu(OAc)_2$	150	40/48	37
3	OMe	Ph	Cu/Al_2O_3	150	70/48	38
5	H	COOBu	Cu/PrePAN fiber mats	130	99/40	40
6	H	Ph	Pd/Cu (4:1) bimetallic NPs	100	91/18	42

[a] Conversion.

In summary, we have presented a simple procedure for preparing a magnetically recoverable copper catalyst with high efficiency for Mizoroki–Heck and Suzuki–Miyaura cross-coupling reactions with low price for industrial applications. The catalyst showed good diversity and generality in both reactions. This method requires remarkably small amounts of catalyst without any activator or any toxic ligand. The superparamagnetic nature of the catalyst provides its easy isolation and reuse. In addition, high activity and selectivity, easy separation of catalysts, and good performance in the recycling reaction are the valuable advantages of this Fe_3O_4@SiO_2–Isa Cu(II) catalyst.

Table 6. Comparison of the catalytic activity of various heterogeneous catalysts in the Suzuki–Miyaura cross-coupling reaction.

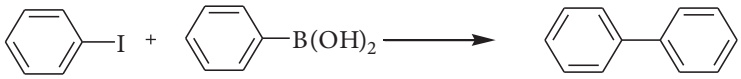

Entry	Catalyst	Temperature (°C)	Yield (%)	Ref.
1	Fe_3O_4@SiO_2–Isa Cu(II)	70	92[a]	This work
2	Cu nanocolloid	110	62	39
3	3D MOF$\{[Cu(4\text{-}tba)_2](solvent)\}_n$	25	88	41
4	Cu-Pd bimetallic catalysts supported on 4Å molecular sieve	78	>99	43
5	Cu, monometallic catalysts supported on 4Å molecular sieve	78	62[a]	43
6	Pd-Cu/C	78	97.5	44

[a]Conversion.

3. Experimental

3-Aminopropyltriethoxysilane (APTES), tetraethyl orthosilicate (TEOS), isatin (Isa), and other chemicals and solvents were purchased from Merck and used as received without further purification. Deionized water was used throughout the experiments. All solvents were of analytical grade. TEM images were carried out using a Philips EM208 at 100 kV. Metal existence, phase purity, and crystallinity of the sample were characterized by XRD using a Philips X'Pert MPD with Cu Kα radiation. The UV-DRS of samples was recorded with a PE Lambda 20 spectrometer. FT-IR spectra were obtained using a Bruker Equinox 55 spectrophotometer. ICP was conducted on a Vista-MPX (Varian) for content determination of copper on supports. Conversion % was determined by GC on a Shimadzu model GC-14A instrument. TGA results were obtained by TA Q50 V6.3. SEM images were carried out on a Hitachi S-4160. EDS data were recorded on a VEGA3 XMU. Magnetic properties of modified MNPs were studied by VSM (Meghnatis Kavir Kashan Co., Kashan, Iran).

3.1. Catalyst preparation

Preparation of Fe_3O_4 nanoparticles: Fe_3O_4MNPs were prepared via the chemical coprecipitation method.[45] An aqueous solution (100 mL) of $FeCl_2.4H_2O$ (1.0 g, 5.0 mmol) and $FeCl_3.6H_2O$ (2.6 g, 9.6 mmol) was mixed under nitrogen atmosphere with vigorous stirring, and then NH_4OH (10 mL of 25 wt%, excess) was added dropwise to the solution. The solution was heated to 70 °C and kept at this temperature for 2 h. The resultant black dispersion was cooled and separated from the solution with a permanent magnet and washed several times

with deionized water and ethanol until the pH value held at 7. The precipitate was dried in a vacuum oven at 80 °C for 24 h.

Preparation of Fe_3O_4@SiO_2 nanoparticles: Fe_3O_4 MNPs (0.7 g) were dispersed in a mixture of ethanol (40 mL) and deionized water (10 mL). To this dispersion, TEOS (0.3 mL) and NH_4OH (0.6 mL) were added and the mixture was stirred vigorously at room temperature for 12 h. Silica-coated MNPs were magnetically isolated by a permanent magnet, repeatedly washed with ethanol and deionized water, and finally dried in a vacuum at 50 °C for 24 h.[46]

General procedure for preparation of amine functionalized MNPs (Fe_3O_4@SiO_2–NH_2) : presynthesized Fe_3O_4@SiO_2 MNPs (1.0 g) were well dispersed in anhydrous toluene and then an excess amount of 3-aminopropyltriethoxysilane (0.7 mL, 0.66 g) was added dropwise to this dispersion. The mixture was refluxed for 24 h under argon protection. The resulting amine functionalized MNPs were magnetically separated by external magnet, washed with methanol and acetone several times, and dried in a vacuum oven at 50 °C overnight.[47]

Preparation of isatin functionalized MNPs (Fe_3O_4@SiO_2–Isa): the appropriate Schiff base was prepared by condensation reaction of Fe_3O_4@SiO_2–NH_2 with isatin. The solution of isatin (10 mmol) in ethanol (25 mL) was added dropwise to the dispersed Fe_3O_4@SiO_2–NH_2 nanoparticles (1.0 g) in ethanol (25 mL). The resulting mixture was refluxed under argon atmosphere for 24 h. The product was collected by an external magnet and carefully washed with ethanol. Subsequently, it was treated by Soxhlet extraction with ethanol for 24 h to remove unreacted substrates and byproducts and finally dried at 50 °C overnight in a vacuum oven.

Preparation of copper loading on Fe_3O_4@SiO_2–Isa MNPs (Fe_3O_4@SiO_2–Isa Cu(II)): the immobilized Schiff base (300 mg) and copper acetate (0.6 mmol) were dispersed in acetonitrile (80 mL) under sonication for 30 min. The mixture was stirred vigorously for 24 h under argon at room temperature. The magnetic catalyst was washed with acetone, ethanol, and water several times and dried under a vacuum at room temperature to yield the immobilized copper Schiff base complex.

3.2. General procedure for Heck coupling reaction

A mixture of aryl iodide (1.0 mmol), methyl acrylate (1.1 mmol), triethylamine (2.0 mmol), and an adequate amount of copper catalyst (0.33 mol%) was taken in a round-bottom flask and stirred in DMF (5.0 mL) at 100 °C, and the progress of the reaction was monitored by GC.[48] At the end of the reaction, the mixture was cooled to room temperature and the catalyst was isolated by magnetic decantation. The recovered catalyst was thoroughly rinsed with ethyl acetate and distilled water, dried at room temperature, and used without any pretreatment for the next runs. The recyclability of the catalyst was screened in the reaction between iodobenzene and methyl acrylate according to the above procedure.

3.3. General procedure for Suzuki coupling reaction

The mixture of aryl iodide (1.0 mmol), phenyl boronic acid (1.1 mmol), potassium carbonate (2.0 mmol), and copper catalyst (0.33 mol%) was taken in a round-bottom flask and stirred in ethanol (5.0 mL) under reflux conditions (70 °C), and the progress of the reaction was monitored by GC.[49] At the end of the reaction, the mixture was cooled to room temperature and the solid catalyst was isolated by magnetic decantation. The recyclability of the catalyst was screened in the reaction between iodoanisole and phenylboronic acid according to the same method described above.

Acknowledgment

This work was supported by grants from the Research Council of Tehran University of Medical Science.

References

1. Trzeciak, A. M.; Ziółkowski, J. *J. Coord. Chem. Rev.* **2005**, *249*, 2308–2322.
2. Farina, V. *Adv. Synth. Catal.* **2004**, *346*, 1553–1582.
3. Mizutani, T.; Honzawa, S.; Tosaki, S. Y.; Shibasaki, M. *Angew. Chem. Int. Ed.* **2002**, *41*, 4680–4682.
4. Díez-González, S.; Nolan, S. P. *Top. Organomet. Chem.* **2007**, *21*, 47–82.
5. Choudary, B. M.; Madhi, S.; Chowdari, N. S.; Kantam, M. L.; Sreedhar, B. *J. Am. Chem. Soc.* **2002**, *124*, 14127–14136.
6. Häberli, A.; Leumann, C. J. *Org. Lett.* **2001**, *3*, 489–492.
7. Makhubela, B. C.; Jardine, A.; Smith, G. S. *Appl. Catal. A-Gen.* **2011**, *393*, 231–241.
8. Iranpoor, N.; Firouzabadi, H.; Motevalli, S.; Talebi, M. *J. Organomet. Chem.* **2012**, *708*, 118–124.
9. Yuan, D.; Zhang, Q.; Dou, J. *Catal. Commun.* **2010**, *11*, 606–610.
10. Costa, N. J.; Kiyohara, P. K.; Monteiro, A. L.; Coppel, Y.; Philippot, K.; Rossi, L. M. *J. Catal.* **2010**, *76*, 382–389.
11. Mao, J.; Guo, J.; Fang, F.; Ji, S. J. *Tetrahedron* **2008**, *64*, 3905–3911.
12. Calò, V.; Nacci, A.; Monopoli, A.; Ieva, E.; Cioffi, N. *Org. Lett.* **2005**, *7*, 617–620.
13. Liu, Y.; Li, D.; Park, C. M. *Angew. Che. Int. Ed.* **2011**, *50*, 7333–7336.
14. Gigant, N.; Gillaizeau, I. *Org. Lett.* **2012**, *14*, 3304–3307.
15. Ko, S.; Jang, J. *Angew. Chem. Int. Ed.* **2006**, *45*, 7564–7567.
16. Cui, J.; He, T.; Zhang, X. *Catal. Commun.* **2013**, *40*, 66–70.
17. Phan, N. T.; Le, H. V. *J. Mol. Catal. A-Chem.* **2011**, *334*, 130–138.
18. Zamani, F.; Hosseini, S. M. *Catal. Commun.* **2014**, *43*, 164–168.
19. Beygzadeh, M.; Alizadeh, A.; Khodaei, M.; Kordestani, D. *Catal. Commun.* **2013**, *32*, 86–91.
20. Dehghani, F.; Sardarian, A. R.; Esmaeilpour, M. *J. Organomet. Chem.* **2013**, *743*, 233–240.
21. Taher, A.; Kim, J. B.; Jung, J. Y.; Ahn, W. S.; Jin, M. J. *Synlett* **2009**, *15*, 2477–2482.
22. Tamizh, M. M.; Karvembu, R. *Inorg. Chem. Commun.* **2012**, *25*, 30–34.
23. Monier, M.; Ayad, D.; Wei, Y.; Sarhan, A. *J. Hazard. Mater.* **2010**, *177*, 962–970.
24. Lagasi, M.; Moggi, P. *J. Mol. Catal. A-Chem.* **2002**, *183*, 61–72.
25. Zhu, M.; Diao, G. *J. Phys. Chem. C* **2011**, *115*, 24743–24749.
26. Deng, Y.; Qi, D.; Deng, C.; Zhang, X.; Zhao, D. *J. Am. Chem. Soc.* **2008**, *130*, 28–29.
27. Wang, B.; Wu, X. L.; Shu, C. Y.; Guo, Y. G.; Wang, C. R. *J. Mat. Chem.* **2010**, *20*, 10661–10664.
28. Qadir, M.; Möchel, T.; Hii, K. K. *Tetrahedron* **2000**, *56*, 7975–7979.
29. Zhang, M.; Shao, C.; Guo, Z.; Zhang, Z.; Mu, J.; Cao, T.; Liu, Y. *ACS Appl. Mater. Interfaces* **2011**, *3*, 369–377.
30. Irie, H.; Miura, S.; Kamiya, K.; Hashimoto, K. *Chem. Phys. Lett.* **2008**, *457*, 202–205.
31. Lee, S. S.; Bai, H.; Liu, Z.; Sun, D. D. *Water Res.* **2013**, *47*, 4059–4073.
32. Arifin, S. A.; Jalaludin, S.; Djaja, N. F.; Saleh, R. *Adv. Mater. Res.* **2015,** *1112*, 221–227.
33. Bagherzadeh, M.; Ashouri, F.; Hashemi, L.; Morsali, A. *Inorg. Chem. Commun.* **2014**, *44*, 10–14.
34. Amini, M.; Bagherzadeh, M.; Rostamnia, S. *Chin. Chem. Lett.* **2013**, *24*, 433–436.
35. Wu, Q.; Wang, L. *Synthesis* **2008**, *2008*, 2007–2012.

36. Zhang, T. Y.; Allen, M. J. *Tetrahedron Lett.* **1999**, *40*, 5813–5816.
37. Yang, Y.; Zhou, R.; Zhao, S.; Li, Q.; Zheng, X. *J. Mol. Catal. A-Chem.* **2003**, *192*, 303–306.
38. Iyer, S.; Thakur, V. V. *J. Mol. Catal. A-Chem.* **2000**, *157*, 275–278.
39. Thathagar, M. B.; Beckers, J.; Rothenberg, G. *J. Am. Chem. Soc.* **2002**, *124*, 11858–11859.
40. Shao, L.; Qi, C. *Appl. Catal. A-Gen.* **2013**, *468*, 26–31.
41. Wang, B.; Yang, P.; Ge, Z. W.; Li, C. P. *Inorg. Chem. Commun.* **2015**, *61*, 13–15.
42. Heshmatpour, F.; Abazari, R.; Balalaie, S. *Tetrahedron* **2012**, *68*, 3001–3011.
43. Fodor, A.; Hell, Z.; Pirault-Roy, L. *Appl. Catal. A-Gen.* **2014**, *484*, 39–50.
44. Kim, S. J.; Oh, S. D.; Lee, S.; Choi, S. H. *J. Ind. Eng. Chem.* **2008**, *14*, 449–456.
45. Xue, X.; Wang, J.; Mei, L.; Wang, Z.; Qi, K.; Yang, B. *Colloid Surface B* **2013**, *103*, 107–113.
46. Deng, Z.; Wei, J.; Xue, X.; Wang, J.; Chen, L. *J. Porous Mat.* **2001**, *8*, 37–42.
47. Jiang, Y.; Jiang, J.; Gao, Q.; Ruan, M.; Yu, H.; Qi, L. *Nanotechnology* **2008**, *19*, 75714–75720.
48. Kamal, A.; Srinivasulu, V.; Seshadri, B. N.; Markandeya, N.; Alarifi, A.; Shankaraiah, N. *Green Chem.* **2012**, *14*, 2513–2522.
49. Gao, Z.; Feng, Y.; Cui, F.; Hua, Z.; Zhou, J.; Zhu, Y.; Shi, J. *J. Mol. Catal. A-Chem.* **2011**, *336*, 51–57.